AIP Advances

# A comparative study of hydrostatic pressure treated environmentally friendly perovskites $CsXBr_3$ (X = Ge/Sn) for optoelectronic applications

Cite as: AIP Advances **11**, 075109 (2021); https://doi.org/10.1063/5.0057287
Submitted: 19 May 2021 • Accepted: 21 June 2021 • Published Online: 06 July 2021

M. A. Islam, Md. Zahidur Rahaman and Sapan Kumar Sen

# A comparative study of hydrostatic pressure treated environmentally friendly perovskites $CsXBr_3$ (X = Ge/Sn) for optoelectronic applications

Cite as: AIP Advances 11, 075109 (2021); doi: 10.1063/5.0057287
Submitted: 19 May 2021 • Accepted: 21 June 2021 •
Published Online: 6 July 2021



M. A. Islam,[1,a] Md. Zahidur Rahaman,[2] and Sapan Kumar Sen[3]

## AFFILIATIONS

[1] Department of Physics, University of Barishal, Barishal 8200, Bangladesh
[2] School of Materials Science and Engineering, Faculty of Science, University of New South Wales, Sydney 2052, Australia
[3] Institute of Electronics, Atomic Energy Research Establishment, Bangladesh Atomic Energy Commission, Dhaka 1349, Bangladesh

[a] **Author to whom correspondence should be addressed:** arifphy6@gmail.com and mauislam@bu.ac.bd. **Present address**: Department of Physics, University of Barishal, Barishal 8200, Bangladesh. **Tel.:** +88 0155 8739718

## ABSTRACT

All-inorganic cubic cesium germanium bromide ($CsGeBr_3$) and cesium tin bromide ($CsSnBr_3$) perovskites have attracted much attention because of their outstanding optoelectronic properties that lead to many modern technological applications. During their evolution process, it can be helpful to decipher the pressure dependence of structural, optical, electronic, and mechanical properties of $CsXBr_3$ (X = Ge/Sn) based on *ab initio* simulations. The lattice parameter and unit cell volume have been decreased by applying pressure. This study reveals that the absorption peak of $CsXBr_3$ (X = Ge/Sn) perovskites is radically changed toward the lower photon energy region with the applied pressure. In addition, the conductivity, reflectivity, and dielectric constant have an increasing tendency under pressure. The study of electronic properties suggested that $CsXBr_3$ (X = Ge/Sn) perovskites have a direct energy bandgap. It is also found through the study of mechanical properties that $CsXBr_3$ (X = Ge/Sn) perovskites are ductile under ambient conditions and their ductility has been significantly improved with pressure. The analysis of bulk modulus, shear modulus, and Young's modulus reveals that hardness of $CsXBr_3$ (X = Ge/Sn) perovskites has been enhanced under external pressure. These outcomes suggest that pressure has a significant effect on the physical properties of $CsXBr_3$ (X = Ge/Sn) perovskites that might be promising for photonic applications.



## I. INTRODUCTION

Pressure plays a vital role in tuning the physical properties of materials.[1–8] For instance, recently, room temperature superconductors have been discovered at higher pressure.[9] Pressure treated phase transitions are often reversible if the external condition remains exactly the same in the cycle.[10–15] For that reason, pressure-driven paths that may get novel conditions with good ambient equilibrium are very crucial. High pressure studies sometimes offer fundamental insight into the optoelectronic properties of perovskite materials.[16–22] Being an advanced class of substances that have exhibited great potential in optoelectronic technologies, usually utilized in solar cells and thin-film transistors, the rapidly growing all-inorganic lead-free perovskites have an extremely versatile crystal structure.[23–25] The growing worldwide demand for electricity and continuing reductions in fossil fuel-based energy sources forecast the increased use of renewable energy resources. Solar power, one of the potential renewable sources of electricity, has become the most promising source, since it could be transformed into electric energy and reach nearly every area of the Earth.[26,27] Lately, lead-based halide perovskites reveal outstanding optoelectronic properties, but out of the perspective of environmental issues, their lead content is deemed to be problematic.[28,29] To address the toxicity problem, the study of lead-free perovskite materials is becoming livelier, such as bismuth halide perovskites, germanium halide perovskites, copper halide perovskites, and tin halide perovskites.[30–39]

Specifically, germanium and tin halide perovskites are attracting much attention as they have attained relatively high solar cell efficiencies.[40–45] The excellent optoelectronic characteristics of perovskite absorbers, such as powerful light absorption and cheap production, have encouraged perovskite solar cells to eventually turn into one of the very promising photovoltaic technologies toward rapid commercialization.[46–49]

Many researchers have explored lead-free halide perovskites. Lately, Roknuzzaman *et al.* investigated the structural, mechanical, and electronic properties of $CsGeBr_3$ and $CsSnBr_3$ perovskites.[40] According to the present information, no literature can be found on pressure treated cubic $CsXBr_3$ (X = Ge/Sn) perovskites. Hence, we decide to explore the detailed physical properties of non-toxic perovskites $CsXBr_3$ (X = Ge/Sn) under pressure by the *ab initio* approach. It is nevertheless obvious that non-toxic perovskites, alternate to lead-based perovskites, are essential for their market approval.

## II. COMPUTATIONAL METHODS

The first-principles calculation based on density functional theory (DFT) and the plane wave pseudo-potential procedure implemented by the Cambridge Sequential Total Energy Package (CASTEP) code are all utilized in this calculation.[50–52] The interaction among ions and electrons is described by the ultrasoft pseudo-potential, whereas the exchange correlation functional in between electrons is treated as Perdew–Burke–Ernzerhof (PBE) in generalized gradient approximation (GGA).[53,54] The BFGS (Broyden–Fletcher–Goldfarb–Shanno) technique is utilized to optimize the structure.[55] We fixed the plane wave energy cutoff of these systems at 550 eV, the Monkhorst–Pack scheme is utilized for the structural relaxations, and also the k-point grid is set as 12 × 12 × 12.[56] The obtained elastic constants were computed by employing the finite strain theory that was used in the CASTEP module. For the optimum value, the maximum strain amplitude was selected as 0.003. The convergence threshold of total energy is fixed as $5 \times 10^{-6}$ eV/atom, the convergence threshold of the maximum forces between atoms is fixed as 0.01 eV/Å, the convergence threshold of maximum displacement of atoms is fixed as $5 \times 10^{-4}$ Å, and the convergence threshold of crystal internal stress is fixed as 0.02 GPa.

## III. RESULTS AND DISCUSSION

### A. Structural properties

At room temperature, the family of non-toxic Ge/Sn-based halide perovskites $CsXBr_3$ (X = Ge/Sn) belongs to the cubic structure system having space group $Pm\bar{3}m$ (no. 221) as shown in Fig. 1.[57,58] The unit cell of these crystals has five atoms with one formula unit. In a unit cell of cubic $CsXBr_3$ (X = Ge/Sn), one type of Cs atom sits at 1a (0, 0, 0), the other Ge/Sn atoms occupy 1b (0.5, 0.5, 0.5), and Br atoms sit at 3c (0, 0.5, 0.5).[40] The pressure-dependent lattice constants and volumes of the Ge/Sn-based halide along with other available experimental and theoretical data are shown in Table I. From the table, it is clear that our calculated results are consistent with experimental as well as previous theoretical results. In this study, the *ab initio*-based DFT simulation has been carried out at various applied pressures from 0 to 6 GPa with a step of 2 GPa.

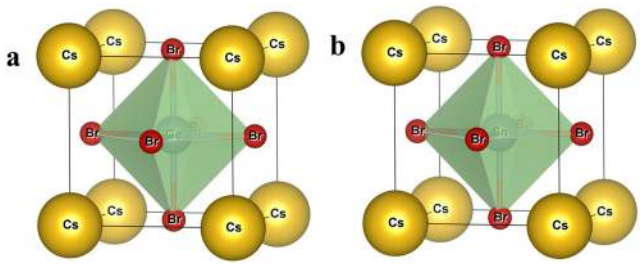


**FIG. 1.** The constructed cubic crystal structure of (a) $CsGeBr_3$ and (b) $CsSnBr_3$.

The effect of applied pressures on lattice parameters and cell volumes is shown in Fig. 2. When the pressure increases, the lattice parameters and cell volumes are found to be decreased as shown in Fig. 2.

### B. Optical properties

The analysis of the optical properties of $CsXBr_3$ (X = Ge/Sn) is quite significant because of their potential to be used in optoelectronics. For this reason, we studied the optical absorption, conductivity, reflectivity, and the real and imaginary parts of the dielectric function of these materials at different applied pressures up to 6 GPa. The performance of solar cells is determined by various optical properties, one of the crucial properties of which is the absorption coefficient. The variation of optical absorption of $CsXBr_3$ (X = Ge/Sn) perovskites with pressure can be seen in Fig. 3. It is clear that the optical absorption edge of cubic $CsXBr_3$ (X = Ge/Sn) perovskites is shifted to the low energy region with applied pressure within the visible ranges. In Fig. 3(a) as compared to Fig. 3(b), absorption edges are remarkably enhanced under pressure within visible ranges. In addition, it is observed that the pressure-dependent absorption coefficient of the Ge-based compound shows maximum intensity in the ultraviolet region relative to Sn-based compounds. The width of the

**TABLE I.** The computed and the available experimental and theoretical values of lattice constant *a* and the evaluated unit cell volume *V* of $CsXBr_3$ (X = Ge/Sn) at different pressures.

| Pressure (GPa) | Phase | *a* (Å) This work | *a* (Å) Other works | *a* (Å) Experimental | *V* (Å$^3$) |
|---|---|---|---|---|---|
| 0 | $CsGeBr_3$ | 5.587 | 5.587[40] | 5.636[43]<br>5.362[44] | 174.4 |
| | $CsSnBr_3$ | 5.881 | 5.882[40] | 5.804[49]<br>5.800[45] | 203.4 |
| 2 | $CsGeBr_3$ | 5.451 | ··· | ··· | 162.0 |
| | $CsSnBr_3$ | 5.720 | ··· | ··· | 187.1 |
| 4 | $CsGeBr_3$ | 5.350 | ··· | ··· | 153.1 |
| | $CsSnBr_3$ | 5.603 | ··· | ··· | 175.9 |
| 6 | $CsGeBr_3$ | 5.268 | ··· | ··· | 146.2 |
| | $CsSnBr_3$ | 5.510 | ··· | ··· | 167.3 |

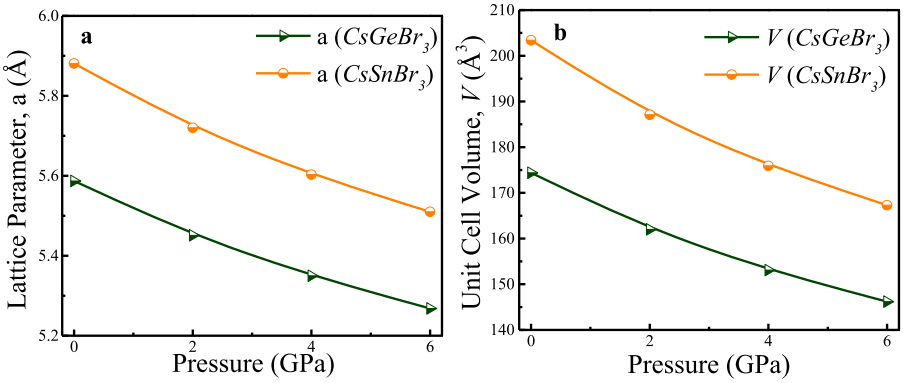


**FIG. 2.** The pressure-dependent (a) lattice parameter and (b) unit cell volume of cubic $CsXBr_3$ (X = Ge/Sn) perovskites.

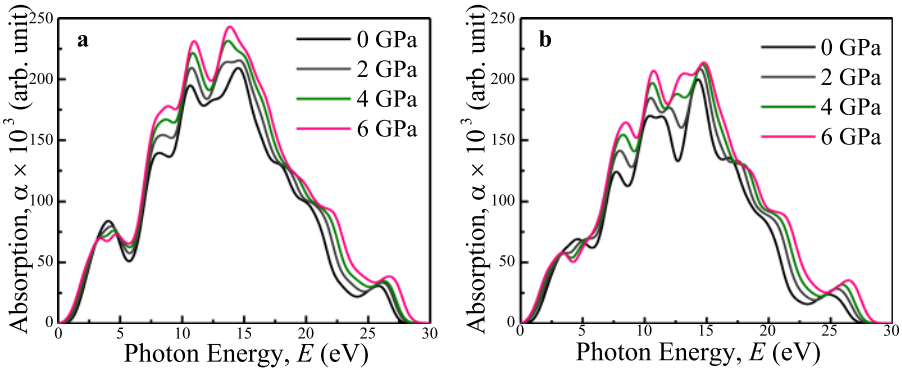


**FIG. 3.** The light absorption spectra of (a) $CsGeBr_3$ and (b) $CsSnBr_3$ at hydrostatic pressures.

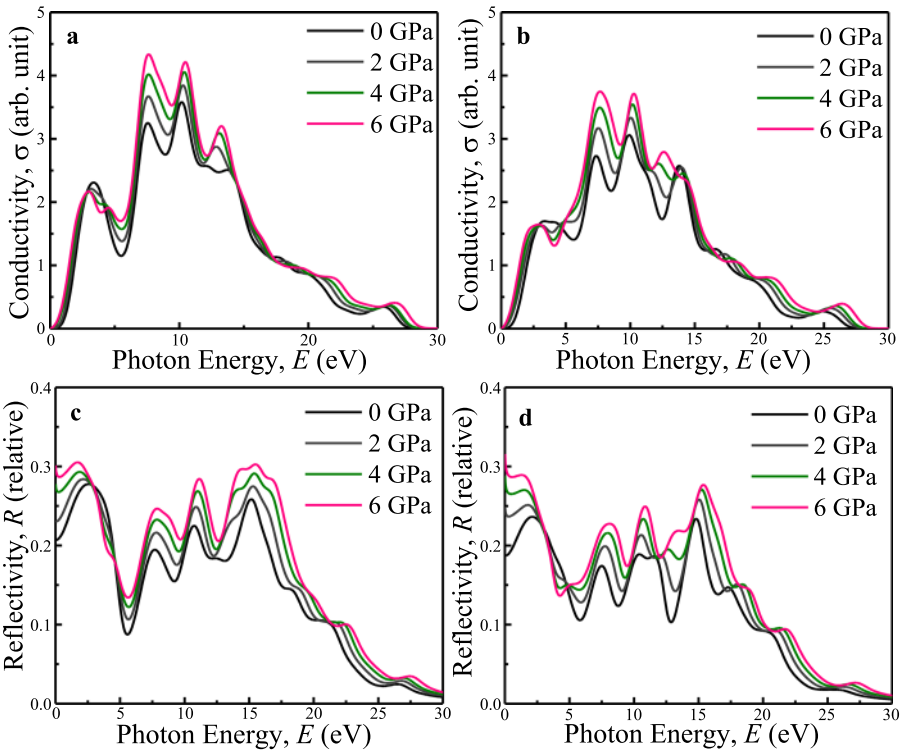


**FIG. 4.** The computed pressure-dependent conductivity of the (a) $CsGeBr_3$ and (b) $CsSnBr_3$; pressure-dependent reflectivity of (c) $CsGeBr_3$ and (d) $CsSnBr_3$.

absorption peak in Fig. 3(a) is higher than in Fig. 3(b) in the UV region. Another name of photoconductivity is optical conductivity.[59,60] The pressure-dependent real part of optical conductivity is shown in Figs. 4(a) and 4(b). If the absorption of photons improves, the rate of photoconductivity tends to increase. As a result, we observed greater absorption as well as more photoconductivity in the Ge-based compound relative to the Sn-based compound with applied pressures.

Reflectivity that determines the surface nature of the perovskite materials is also another important optical property of the solar cell.[61] Figures 4(b) and 4(c) show the reflectivity spectra for various applied pressures. Here, all the studied cubic perovskite compounds show low reflectivity but slightly increased nature with pressure.

The dielectric function of the solar cell is a fundamental parameter related to the charge-carrier regeneration rate of certain materials.[62,63] The dielectric function gives a clear idea of performance of optoelectronic devices.[64] In the perovskite solar cells, higher dielectric constant values cause lower recombination rates. Figure 5 shows the pressure dependence of the dielectric constant (real and imaginary parts) of non-toxic $CsXBr_3$ (X = Ge/Sn) perovskites. The real part of the dielectric constant is shown in Figs. 5(a) and 5(b). The values are high at low photon energy and then decrease rapidly with increase in photon energy. In the visible range, the pressure-induced sample exhibits a higher dielectric constant. Normally, the perovskite material with such a higher value of the dielectric constant exhibits a lower bandgap.[38] It is also seen in Fig. 6. The plots of the imaginary part of the dielectric constant with pressure are depicted in Figs. 5(c) and 5(d). The behavior of the imaginary part correlated with the optical absorption and material's bandgap.

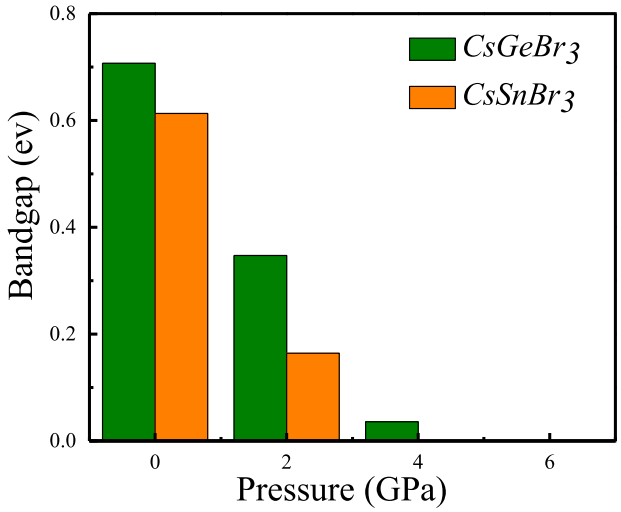


**FIG. 6.** The bandgap of $CsXBr_3$ (X = Ge/Sn) at different hydrostatic pressures.

In the visible range, the values of the imaginary part of the dielectric function are found to be enhanced with applied pressure and the peaks are shifted to a low photon energy region similar to optical absorption in Figs. 5(c) and 5(d). In the higher photon energy region, each imaginary part of the dielectric function decreases to zero.

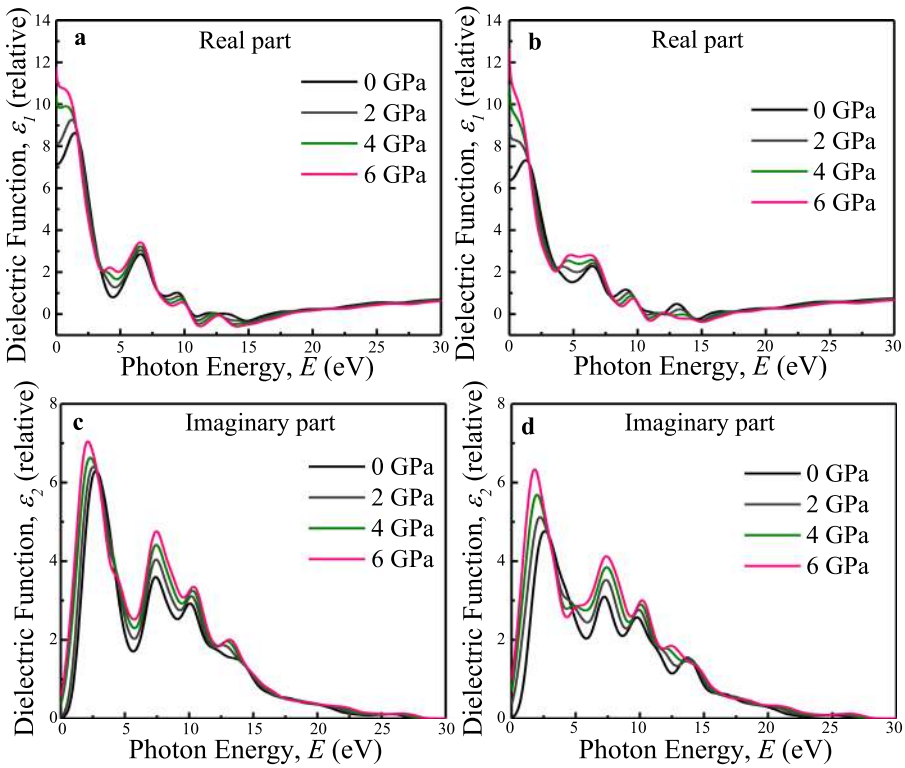


**FIG. 5.** The pressure-dependent real part of the dielectric function of (a) $CsGeBr_3$ and (b) $CsSnBr_3$ and the pressure-dependent imaginary part of the dielectric function of (c) $CsGeBr_3$ and (d) $CsSnBr_3$.

This is because optical absorption in both compounds is very low in the high photon energy region.

### C. Electronic properties

For better insight into the physical properties of materials, the study of the density of states (DOS) and electrical band structure is critical. In Fig. 6, we analyze the changes in the bandgap of $CsXBr_3$ (X = Ge/Sn) at various pressures. When no hydrostatic pressure is applied, the bandgap values of the two compounds ($CsGeBr_3$ and $CsSnBr_3$) are 0.707 and 0.613 eV, respectively, which are very comparable to other theoretical results.[40] By using the GGA and PBE, we have evaluated the electronic bandgap.[65] Moreover, our estimated bandgaps for $CsXBr_3$ (X = Ge/Sn) are smaller than those found in the experimental study. The explanation for this has been attributed to GGA's well-known limitation.[66] We found that the elevated pressure from 0 to 6 GPa leads to the gradual decrease in bandgaps for both the compounds as shown in Fig. 7.

The direct bandgap vanished at the R-point with applied hydrostatic pressure. At 6 GPa pressure, the electrical bandgap of the $CsGeBr_3$ perovskite vanished, while the electrical bandgap of the $CsSnBr_3$ perovskite vanished at 4 GPa. As a result, the valence band and the conduction band overlap and enhance the optical conductivity of metal halides.

In order to better describe the electronic band structure, we looked at density of states (DOS).[67] As shown in Fig. 8, we portrayed the total density of states (TDOS) and partial density of states (PDOS) of $CsXBr_3$ (X = Ge/Sn) perovskites at various applied pressures. In the case of $CsGeBr_3$ perovskite under pressure, we see from Fig. 8 that the Br-4*p* orbital contributes the most to the valence band, whereas Cs-5*p*, Ge-4*p*, and Ge-4*s* orbitals play a minor role. The conduction band, on the other hand, was dominated by the Br-4*s* orbital, with slight contributions from the Cs-5*p*, Ge-4*p*, and Ge-4*s* orbitals.

As seen in Fig. 8, the Br-4*p* orbital contributed the most to the valence band of another $CsSnBr_3$ perovskite under the same

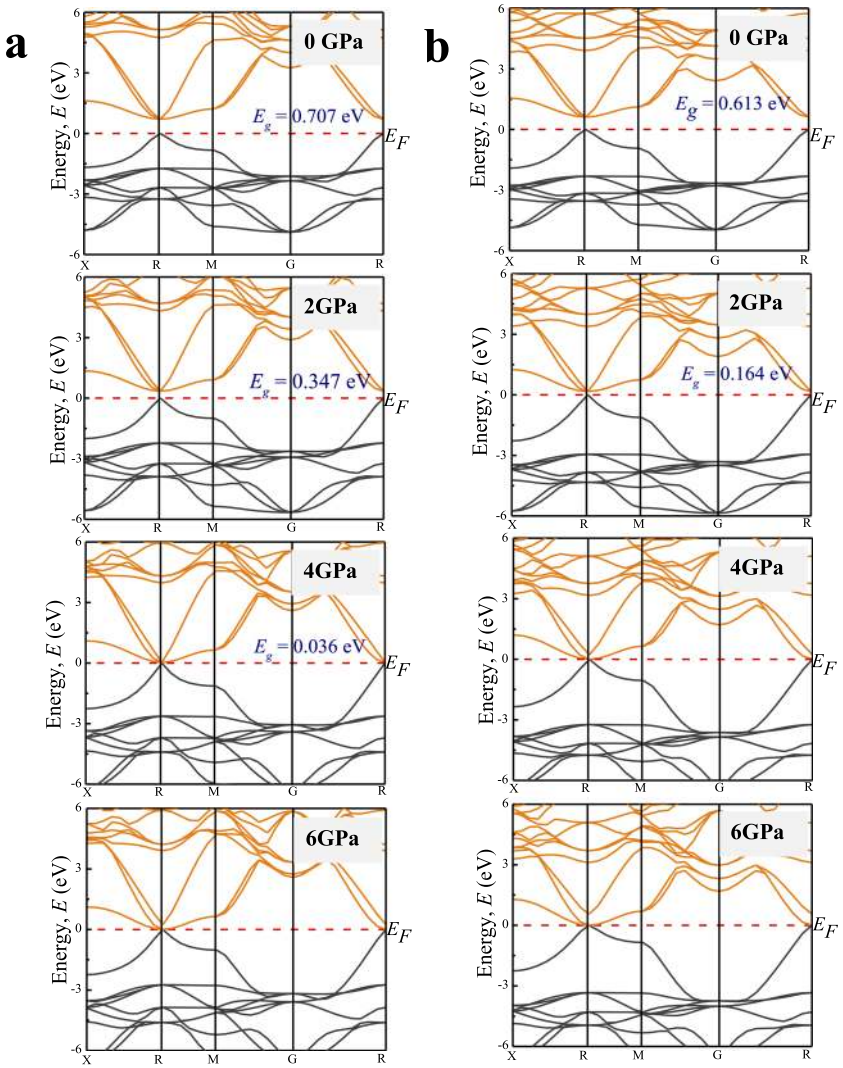


**FIG. 7.** The band structure diagram of (a) $CsGeBr_3$ and (b) $CsSnBr_3$ at various pressures.

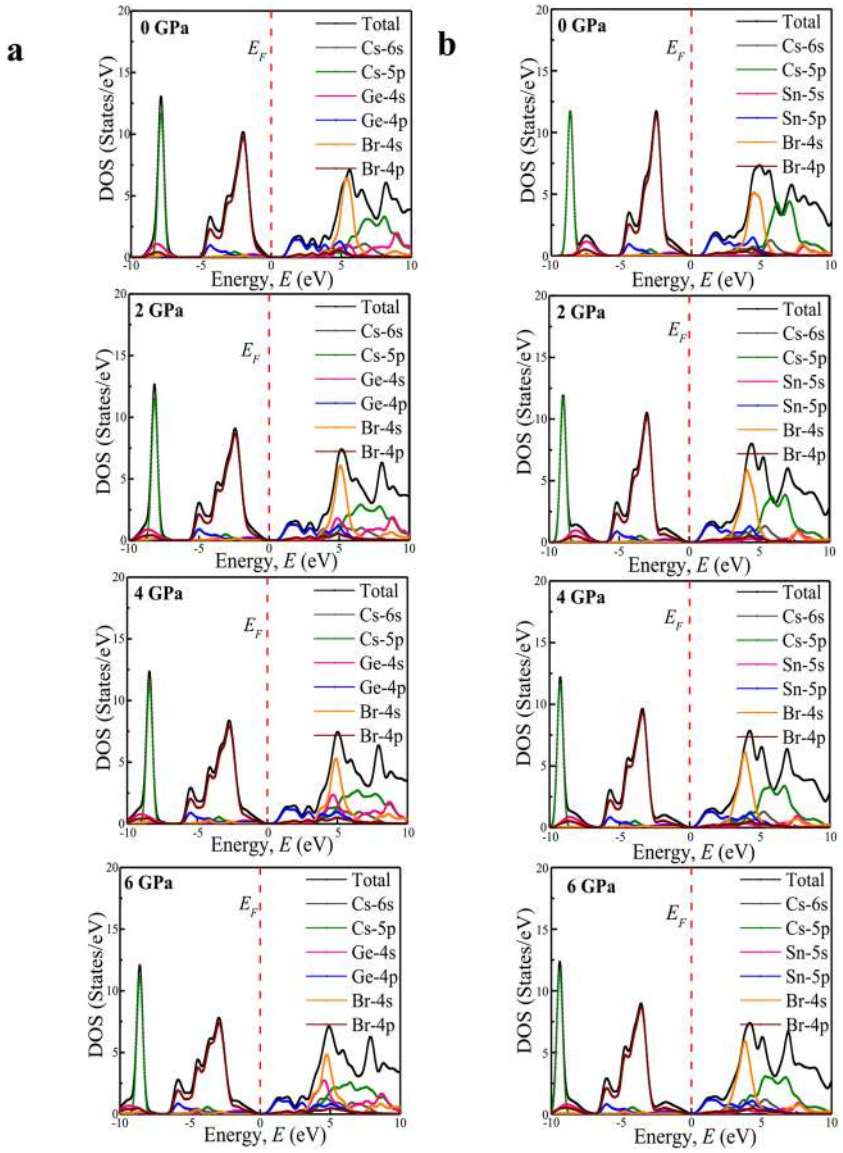


**FIG. 8.** The total density of states (TDOS) and partial density of states (PDOS) of cubic (a) $CsGeBr_3$ and (b) $CsSnBr_3$ under pressure.

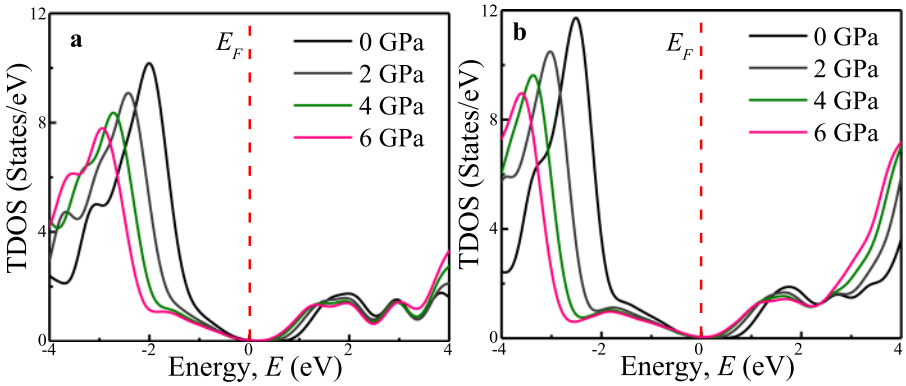


**FIG. 9.** The pressure-dependent TDOS value of (a) $CsGeBr_3$ and (b) $CsSnBr_3$ near the Fermi level.

**TABLE II.** The calculated values of $C_{ij}$ (GPa) and Cauchy pressure $C_{12}$–$C_{44}$ (GPa) of cubic $CsXBr_3$ (X = Ge/Sn) perovskites at various pressures.

| Pressure (GPa) | Phase | $C_{11}$ | $C_{12}$ | $C_{44}$ | $C_{12}-C_{44}$ |
|---|---|---|---|---|---|
| 0[40] | $CsGeBr_3$ | 48.08 | 10.82 | 10.07 | 0.75 |
| | $CsSnBr_3$ | 43.89 | 6.69 | 5.21 | 1.48 |
| 0 | $CsGeBr_3$ | 47.78 | 10.49 | 10.07 | 0.42 |
| | $CsSnBr_3$ | 44.15 | 6.92 | 5.25 | 1.67 |
| 2 | $CsGeBr_3$ | 66.02 | 14.37 | 11.64 | 2.73 |
| | $CsSnBr_3$ | 62.93 | 8.89 | 5.28 | 3.61 |
| 4 | $CsGeBr_3$ | 82.88 | 17.96 | 13.09 | 4.87 |
| | $CsSnBr_3$ | 82.88 | 14.00 | 5.65 | 8.35 |
| 6 | $CsGeBr_3$ | 99.14 | 21.64 | 14.45 | 7.19 |
| | $CsSnBr_3$ | 99.07 | 16.73 | 4.84 | 11.89 |

**TABLE III.** The calculated mechanical properties of $CsXBr_3$ (X = Ge/Sn) at different pressures.

| Pressure (GPa) | Phase | $B$ (GPa) | $G$ (GPa) | $E$ (GPa) | $(B/G)$ | $\nu$ |
|---|---|---|---|---|---|---|
| 0[40] | $CsGeBr_3$ | 23.24 | 12.92 | 32.70 | 1.799 | 0.27 |
| | $CsSnBr_3$ | 19.09 | 8.94 | 23.19 | 2.135 | 0.30 |
| 0 | $CsGeBr_3$ | 22.92 | 12.92 | 32.63 | 1.774 | 0.263 |
| | $CsSnBr_3$ | 19.33 | 8.98 | 23.33 | 2.152 | 0.299 |
| 2 | $CsGeBr_3$ | 31.59 | 16.12 | 41.32 | 1.960 | 0.282 |
| | $CsSnBr_3$ | 26.90 | 10.88 | 28.76 | 2.473 | 0.322 |
| 4 | $CsGeBr_3$ | 39.60 | 19.02 | 49.18 | 2.082 | 0.293 |
| | $CsSnBr_3$ | 36.96 | 12.83 | 34.49 | 2.881 | 0.344 |
| 6 | $CsGeBr_3$ | 47.47 | 21.73 | 56.56 | 2.185 | 0.301 |
| | $CsSnBr_3$ | 44.18 | 13.43 | 36.57 | 3.290 | 0.362 |

pressure. The Cs-5*p*, Sn-5*s*, and Sn-5*p* orbitals played minor roles. The Br-4*s* orbital dominated in the conduction band, with minimal contributions from the Cs-5*p*, Sn-5*p*, and Cs-6*s* orbitals.

Figure 9 illustrates the TDOS of $CsXBr_3$ (X = Ge/Sn) perovskites under pressure for a deeper understanding. The DOS at the Fermi level for $CsGeBr_3$ and $CsSnBr_3$ is seen to be zero below 4 GPa for $CsGeBr_3$ and 2 GPa for $CsSnBr_3$. The current research revealed that the pressure caused a semiconductor to metallic electrical phase transition in both compounds. The results of this study are in good agreement with those of recently reported similar-type metal halide perovskites, confirming the validity of this analysis.[40] However, it should be noted that the GGA process underestimates the bandgap and the observed semiconductor to metallic phase transition could be the result of this GGA error. Further research is needed to clarify this issue precisely.

## D. Mechanical properties

The elastic constants of crystalline materials are essential parameters since they provide substantial information about the mechanical properties of the material along with the internal forces in crystals, stability, and stiffness.[68] It is also known that elastic constants provide strong indication about the capability of the crystal to resist external pressure. Since the lattice parameters decrease with the increase in pressure as shown in Fig. 2, it is quite significant to investigate the effect of pressure onto the elastic constants of these non-toxic $CsXBr_3$ (X = Ge/Sn) perovskites. The non-toxic $CsXBr_3$ (X = Ge/Sn) metal halide perovskites possess three independent elastic constants for the cubic structure, which are $C_{11}$, $C_{12}$, and $C_{44}$. The calculated elastic constants at different pressures are tabulated in Table II. For the cubic phase, mechanical stability depends on the well-known Born stability criteria that are expressed as

$$C_{11} > 0, C_{44} > 0, C_{11} + 2C_{12} > 0, \text{and } C_{11} - C_{12} > 0.$$

As shown in Table II, it is evident that all the studied perovskite phases are mechanically stable at different applied pressures according to the above-mentioned stability criteria. Furthermore, the polycrystalline mechanical properties at ambient pressure as listed in Table III matched well with other reported results, bearing the accuracy of the present calculation.[40] According to Table II, it is seen that when the pressure increases up to 6 GPa for the $CsGeBr_3$ perovskite,

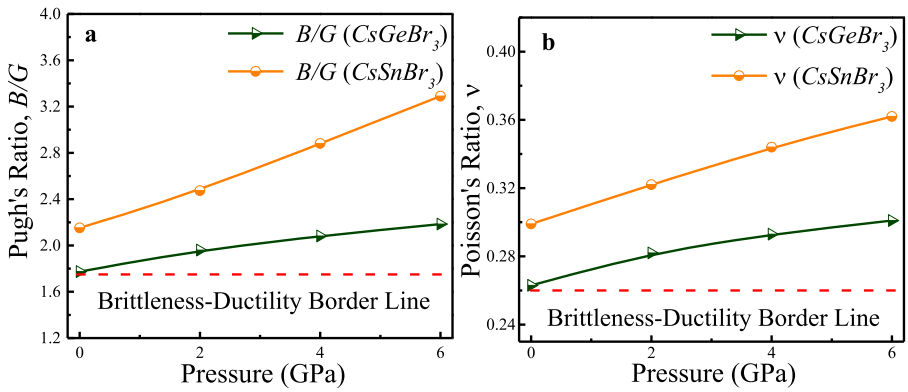


**FIG. 10.** (a) Variation of Pugh's ratio and (b) variation of Poisson's ratio of the $CsXBr_3$ (X = Ge/Sn) perovskite at different pressures.

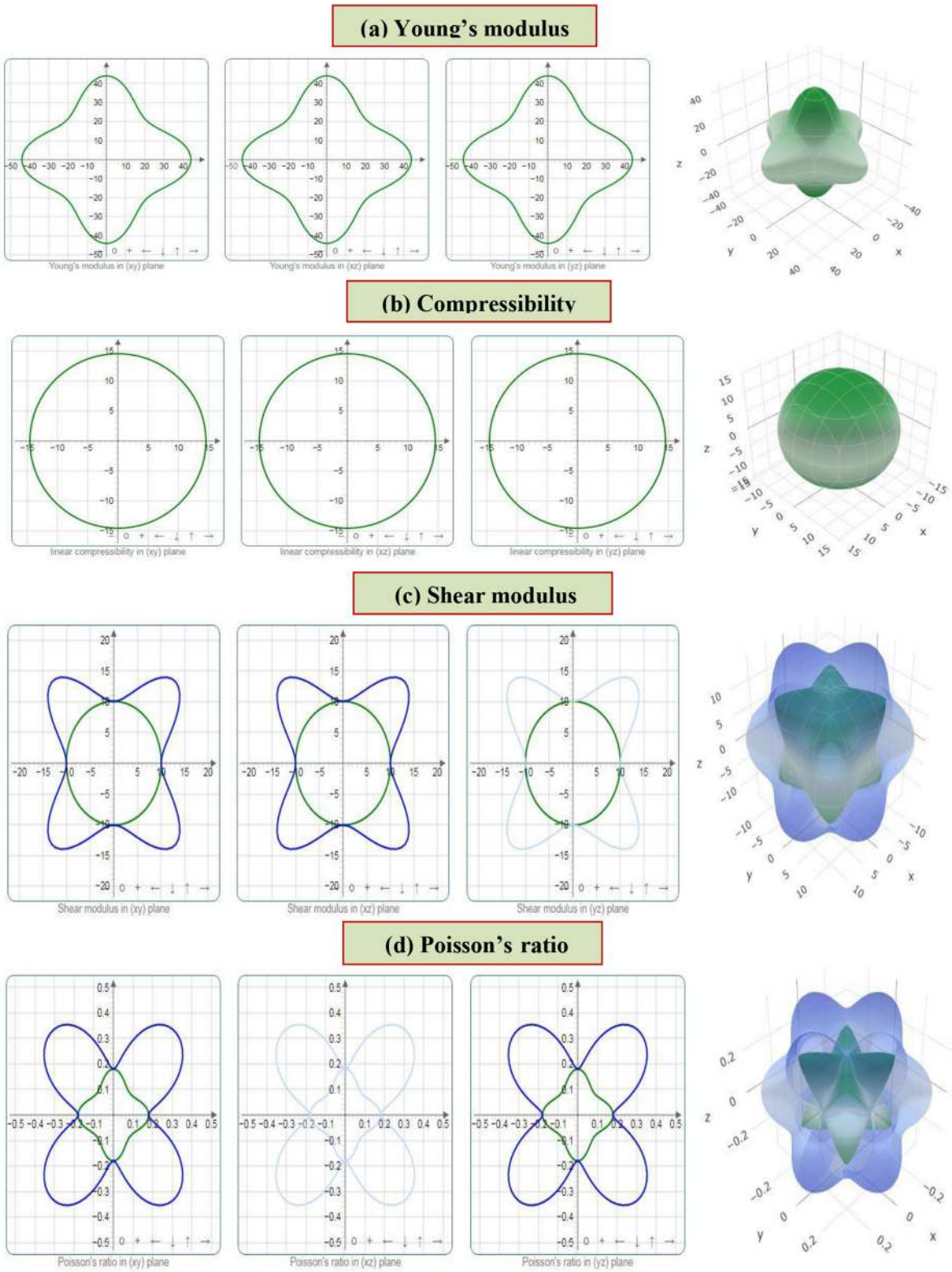


**FIG. 11.** The 2D and 3D plots of (a) Y, (b) K, (c) G, and (d) $\nu$ of $CsGeBr_3$ at 0 GPa.

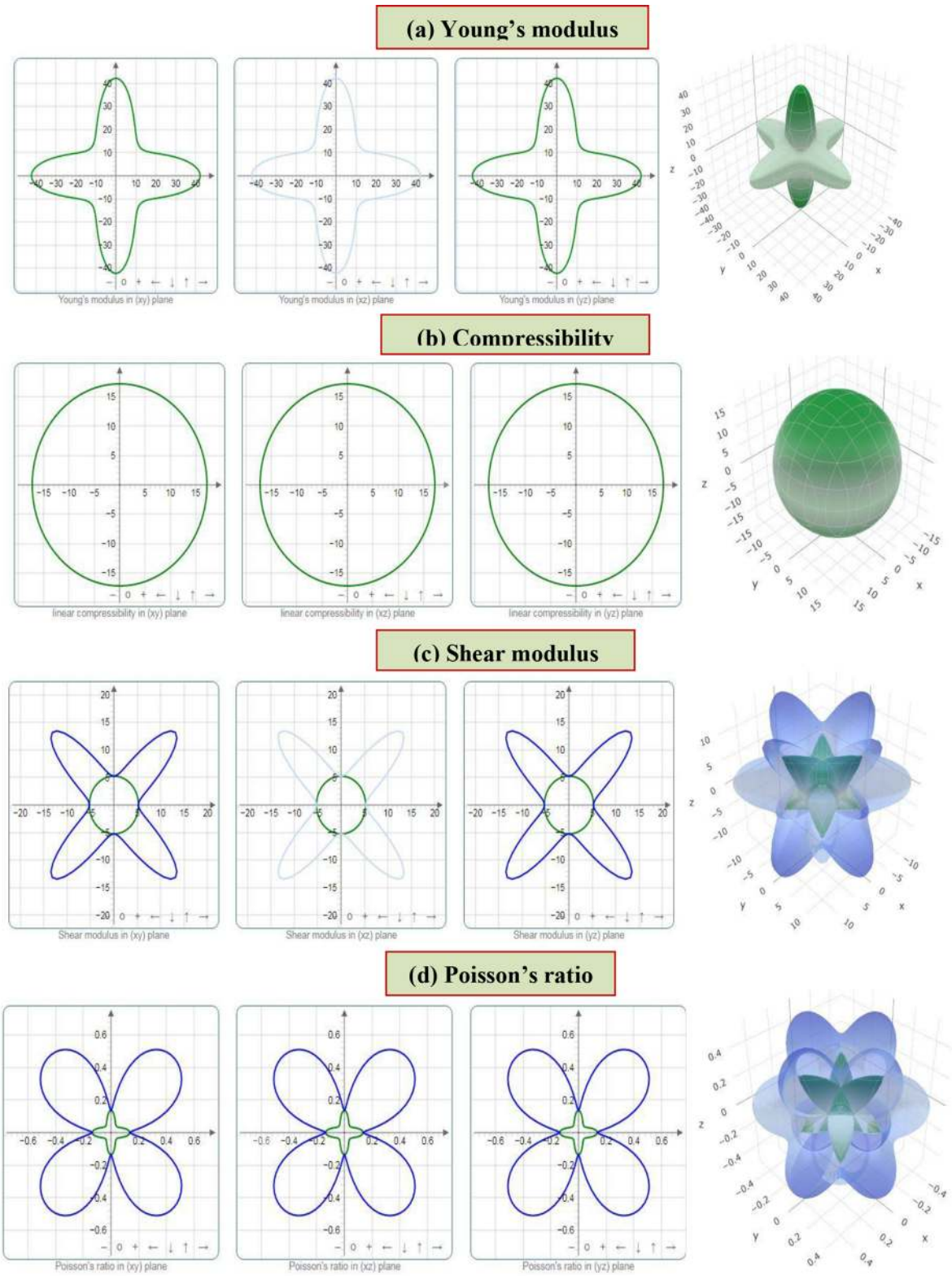


**FIG. 12.** The 2D and 3D plots of (a) Y, (b) K, (c) G, and (d) $\nu$ of $CsSnBr_3$ at 0 GPa.

the values of $C_{44}$ remain unaffected. It is also noticed that the values of $C_{11}$ and $C_{12}$ enhance quickly with increasing pressure.[67] However, the values of $C_{44}$ in the $CsSnBr_3$ perovskite remain nearly constant up to 4 GPa, and the values of $C_{11}$ and $C_{12}$ follow the same trend as $CsGeBr_3$.

In both perovskites, the elasticity of the length has been increased with the increase in pressure, which is associated with two elastic constants $C_{11}$ and $C_{12}$. The elasticity of shape is associated with the $C_{44}$ value that defines the deformation in shape and stiffness. It is evident from Table II that both the compounds have become much stiffer under external pressure. The Cauchy pressure ($C_{12}-C_{44}$) is another useful parameter to signify the ductile and brittle features of substances. When the value of Cauchy pressure is positive (negative), then material indicates ductile (brittle) nature.

It is found from Table II that the values of Cauchy pressure of the non-toxic $CsXBr_3$ (X = Ge/Sn) perovskites are positive at different pressures and also increase with pressure, implying that ductile nature of those perovskites increases with applied pressure. As shown in Table III, the listed mechanical properties, such as shear modulus ($G$), bulk modulus ($B$), Young's modulus ($E$), Poisson's ratio ($\nu$), and Pugh's ratio ($B/G$) of the non-toxic $CsXBr_3$ (X = Ge/Sn) perovskite, are determined with the assistance of equations that were well known as given in the literature.[40]

The cubic $CsXBr_3$ (X = Ge/Sn) perovskites without external pressure show soft nature because of their comparatively small values of $B$, $G$, and $E$. It can be seen from Table III that there is an increasing tendency of $B$, $G$, and $E$ with the applied pressure. It indicates that the hardness of the materials has been improved. Pugh's ratio is also a crucial parameter to signify ductile and brittle behavior of the material. The critical value of Pugh's ratio is 1.7559.[69,70] The brittle nature of a material is revealed below the critical value and the ductile nature of a material is exposed above the critical value. It is seen from Table III that Pugh's ratio of cubic $CsXBr_3$ (X = Ge/Sn) perovskites without applied pressure is larger than the critical value, which shows the ductile nature of the materials. Ductility of the crystals increases with applied pressure, which makes these compounds better for application. Poisson's ratio ($\nu$) is another good standard that offers a better understanding of the bonding forces and stability of the crystal system. The value of Poisson's ratio more than 0.25 and below 0.5 indicates the occurrence of central force in the crystal.[71] From Table III, it can be noticed that the values of Poisson's ratio for the $CsGeBr_3$ perovskite and $CsSnBr_3$ perovskite are 0.263 and 0.299, respectively. These values are significantly lower compared to 0.5 but more than 0.25, implying the occurrence of central forces in both the perovskites. Poisson's ratio has been increased with increasing pressure, but the increasing trend is not significant after 4 GPa, which means that the strong central forces exist in $CsXBr_3$ (X = Ge/Sn). Poisson's ratio can be additionally a helpful index of brittleness and ductility of substances. The critical value of Poisson's ratio is 0.2614, which signifies ductile and brittle behavior of a material. According to Table III, in both perovskites, Poisson's ratio without and with pressure is more than 0.26, which indicates the ductile nature of the studied compounds. The ratio of $B/G$ and $\nu$ of the $CsXBr_3$ (X = Ge/Sn) metal halide with applied pressure is shown in Fig. 10. It is found that the ductility of $CsXBr_3$ (X = Ge/Sn) improves with increased pressure, and thus, applying pressure can be an efficient approach in which large ductility is required to fabricate devices of $CsXBr_3$ (X = Ge/Sn).

Information of anisotropy helps to improve the mechanical performance of a material for various applications.[72,73] In order to evaluate the anisotropy of Young's modulus, compressibility, shear modulus, and Poisson's ratio of the $CsXBr_3$ (X = Ge/Sn) perovskite, we have used the ELATE code to plot the 2D and 3D images of anisotropy as shown in Figs. 11 and 12.[74] The spherical (3D) and circular (2D) nature of the elastic modules reflect the isotropic nature of the solids, while the divergence from the spherical/circular symmetry shows the degree of anisotropy. In all compounds, Young's modulus (Y) is found to be anisotropic in xy, yz, and xz planes, but compressibility (K) is isotropic in xy, yz, and xz planes, as seen in Figs. 11(a), 11(b) and 12(a), 12(b). Figures 11(c) and 12(c) show that shear modules have two surfaces for 2D and 3D presentations. The blue line represents the maximum values for each angle, while the green line shows the minimum values for the same angle. The minimum value and the maximum value are overlapped at the horizontal and vertical axis for each compound, which means all compounds are anisotropic. Similarly, anisotropic properties are found as seen in Figs. 11(d) and 12(d) for $CsXBr_3$ (X = Ge/Sn) compounds. The minimum and maximum values of Y, K, G, and $\nu$ of the $CsXBr_3$ (X = Ge/Sn) cubic perovskite are included in Table IV, which shows that both compounds are elastically anisotropic in nature.

Pressure increases the absorption, photoconductivity, and dielectric properties of the $CsGeBr_3$ compound relative to the $CsSnBr_3$ compound. According to Table V, it is evident that $CsGeBr_3$ is better suited for solar cell devices than $CsSnBr_3$.

**TABLE V.** Comparison of the key properties of cubic $CsXBr_3$ (X = Ge/Sn) perovskites under pressure.

| Properties | $CsGeBr_3$ | $CsSnBr_3$ |
|---|---|---|
| Optical absorption | High in visible<br>High in the<br>UV region | Medium in visible<br>High in the<br>UV region |
| Photoconductivity | High | Medium |
| Dielectric properties | High | Medium |
| Ductility | Medium | High |

**TABLE IV.** The minimum and maximum values of Young's modulus, compressibility, shear modulus, Poisson's ratio, and the ratio A of $CsXBr_3$ (X = Ge/Sn) at 0 GPa.

| Phase | $Y_{min}$ (GPa) | $Y_{max}$ (GPa) | $A_Y$ | $K_{min}$ ($TPa^{-1}$) | $K_{max}$ ($TPa^{-1}$) | $A_K$ | $G_{min}$ (GPa) | $G_{max}$ (GPa) | $A_G$ | $\nu_{min}$ (GPa) | $\nu_{max}$ (GPa) | $A_\nu$ |
|---|---|---|---|---|---|---|---|---|---|---|---|---|
| $CsGeBr_3$ | 26.36 | 44.01 | 1.67 | 14.54 | 14.54 | 1.00 | 10.07 | 18.65 | 1.85 | 0.120 | 0.454 | 3.79 |
| $CsSnBr_3$ | 14.44 | 42.28 | 2.93 | 17.24 | 17.24 | 1.00 | 5.25 | 18.61 | 3.55 | 0.055 | 0.647 | 11.66 |

## IV. CONCLUSIONS

We have used density functional theory-based theoretical tools to analyze the mechanical, electronic, and optical properties of $CsXBr_3$ (Ge/Sn) at various pressures. The calculated results for both the compounds demonstrate a high degree of consistency with experimental evidence. When the pressure rises, optical absorption of both the compounds shifts toward the low energy region (red shift). The optical absorption in the UV region has also been enhanced dramatically with pressure. We also found that the photoconductivity and dielectric properties of the $CsGeBr_3$ compound are significantly higher than those of the $CsSnBr_3$ compound under pressure. Pressure has a significant effect on the electronic bandgap of both the perovskites. As the pressure increases, Poisson's and Pugh's ratios have been increased. However, pressure has more effect on the ductility of the $CsSnBr_3$ perovskite than that of $CsGeBr_3$. From the above characteristics, it is apparent that $CsGeBr_3$ would perform better than the $CsSnBr_3$ perovskite in solar cells and other optoelectronic devices.

## ACKNOWLEDGMENTS

The authors declare no conflict of interest.

## DATA AVAILABILITY

The data that support the findings of this study are available from the corresponding author upon reasonable request.

## REFERENCES

[1] G. Liu, L. Kong, W. Yang, and H.-k. Mao, Mater. Today **27**, 91 (2019).
[2] U. Schwarz, F. Wagner, K. Syassen, and H. Hillebrecht, Phys. Rev. B **53**, 12545 (1996).
[3] Y. Tang, H. Yang, X. Huang, L. Wang, Q. Zhang, and S. W. Or, Ceram. Int. **44**, 11603 (2018).
[4] Y. Ying, X. Luo, and H. Huang, J. Phys. Chem. C **122**, 17718 (2018).
[5] M. Coduri, T. B. Shiell, T. A. Strobel, A. Mahata, F. Cova, E. Mosconi, F. De Angelis, and L. Malavasi, Mater. Adv. **1**, 2840 (2020).
[6] M. Coduri, T. A. Strobel, M. Szafrański, A. Katrusiak, A. Mahata, F. Cova, S. Bonomi, E. Mosconi, F. De Angelis, and L. Malavasi, J. Phys. Chem. Lett. **10**, 7398 (2019).
[7] D. Z. Metin and N. Gaston, Electron. Struct. **1**, 035001 (2019).
[8] M. I. Kholil and M. T. H. Bhuiyan, J. Phys. Chem. Solids **154**, 110083 (2021).
[9] D. Castelvecchi, Nature **586**, 349 (2020).
[10] B. Winkler, V. Milman, and M.-H. Lee, J. Chem. Phys. **108**, 5506 (1998).
[11] D.-K. Seo, N. Gupta, M.-H. Whangbo, H. Hillebrecht, and G. Thiele, Inorg. Chem. **37**, 407 (1998).
[12] Y. Li, J. Liu, P. Zhang, J. Zhang, N. Xiao, L. Yu, and P. Niu, J. Mater. Sci. **55**, 14873 (2020).
[13] A. P. Nayak, S. Bhattacharyya, J. Zhu, J. Liu, X. Wu, T. Pandey, C. Jin, A. K. Singh, D. Akinwande, and J. F. Lin, Nat. Commun. **5**, 3731 (2014).
[14] J.-H. Lee, A. Jaffe, Y. Lin, H. I. Karunadasa, and J. B. Neaton, ACS Energy Lett. **5**, 2174 (2020).
[15] J. Lin, H. Chen, Y. Gao, Y. Cai, J. Jin, A. S. Etman, J. Kang, T. Lei, Z. Lin, M. C. Folgueras, L. N. Quan, Q. Kong, M. Sherburne, M. Asta, J. Sun, M. F. Toney, J. Wu, and P. Yang, Proc. Natl. Acad. Sci. U. S. A. **116**, 23404 (2019).
[16] T. C. Jellicoe, J. M. Richter, H. F. J. Glass, M. Tabachnyk, R. Brady, S. E. Dutton, A. Rao, R. H. Friend, D. Credgington, N. C. Greenham, and M. L. Böhm, J. Am. Chem. Soc. **138**, 2941 (2016).
[17] A. Bernasconi, A. Rizzo, A. Listorti, A. Mahata, E. Mosconi, F. De Angelis, and L. Malavasi, Chem. Mater. **31**, 3527 (2019).
[18] O. V. Oyelade, O. K. Oyewole, D. O. Oyewole, S. A. Adeniji, R. Ichwani, D. M. Sanni, and W. O. Soboyejo, Sci. Rep. **10**, 7183 (2020).
[19] S. Yalameha, P. Saeidi, Z. Nourbakhsh, A. Vaez, and A. Ramazani, J. Appl. Phys. **127**, 085102 (2020).
[20] Y. Huang, L. Wang, Z. Ma, and F. Wang, J. Phys. Chem. C **123**, 739 (2019).
[21] R. Y. Alyoubi, B. M. Raffah, F. Hamioud, and A. A. Mubarak, Mod. Phys. Lett. B **35**, 2150056 (2021).
[22] M. A. Islam, J. Islam, M. N. Islam, S. K. Sen, and A. K. M. A. Hossain, AIP Adv. **11**, 045014 (2021).
[23] Q. Chen, N. De Marco, Y. Yang, T.-B. Song, C.-C. Chen, H. Zhao, Z. Hong, H. Zhou, and Y. Yang, Nano Today **10**, 355 (2015).
[24] W. A. Dunlap-Shohl, Y. Zhou, N. P. Padture, and D. B. Mitzi, Chem. Rev. **119**, 3193 (2019).
[25] L. K. Gao, Y. L. Tang, and X. F. Diao, Appl. Sci. **10**, 5055 (2020).
[26] Q. Mahmood, M. Yaseen, M. Hassan, M. S. Rashid, I. Tlili, and A. Laref, Mater. Res. Express **6**, 045901 (2019).
[27] L. La Notte, L. Giordano, E. Calabrò, R. Bedini, G. Colla, G. Puglisi, and A. Reale, Appl. Energy **278**, 115582 (2020).
[28] R. Nie, R. R. Sumukam, S. H. Reddy, M. Banavoth, and S. I. Seok, Energy Environ. Sci. **13**, 2363 (2020).
[29] M. Llanos, R. Yekani, G. P. Demopoulos, and N. Basu, Renewable Sustainable Energy Rev. **133**, 110207 (2020).
[30] B. Wu, W. Ning, Q. Xu, M. Manjappa, M. Feng, S. Ye, J. Fu, S. Lie, T. Yin, F. Wang, T. W. Goh, P. C. Harikesh, Y. K. E. Tay, Z. X. Shen, F. Huang, R. Singh, G. Zhou, F. Gao, and T. C. Sum, Sci. Adv. **7**, eabd3160 (2021).
[31] Z. Lan, J. Meng, K. Zheng, and I. E. Castelli, J. Phys. Chem. C **125**, 1592 (2021).
[32] D. Moghe, L. Wang, C. J. Traverse, A. Redoute, M. Sponseller, P. R. Brown, V. Bulović, and R. R. Lunt, Nano Energy **28**, 469 (2016).
[33] S. J. Clark, C. D. Flint, and J. D. Donaldson, J. Phys. Chem. Solids **42**, 133 (1981).
[34] J.-C. Zheng, C. H. A. Huan, A. T. S. Wee, and M. H. Kuok, Surf. Interface Anal. **28**, 81 (1999).
[35] M. G. Brik, in *ECS Meeting Abstracts, MA2011-02* (IOP Publishing, 2011), p. 1825.
[36] L. Y. Huang and W. R. L. Lambrecht, Phys. Rev. B **88**, 165203 (2013).
[37] M. Houari, B. Bouadjemi, S. Haid, M. Matougui, T. Lantri, Z. Aziz, S. Bentata, and B. Bouhafs, Indian J. Phys. **94**, 455 (2020).
[38] M. I. Kholil, M. T. H. Bhuiyan, M. A. Rahman, M. S. Ali, and M. Aftabuzzaman, RSC Adv. **11**, 2405 (2021).
[39] C.-G. Ma, V. Krasnenko, and M. G. Brik, J. Phys. Chem. Solids **115**, 289 (2018).
[40] M. Roknuzzaman, K. K. Ostrikov, H. Wang, A. Du, and T. Tesfamichael, Sci. Rep. **7**, 14025 (2017).
[41] A. P. Jaroenjittichai and Y. Laosiritaworn, Ceram. Int. **44**, S161 (2018).
[42] C. Zhang, L. Gao, S. Hayase, and T. Ma, Chem. Lett. **46**, 1276 (2017).
[43] L.-C. Tang, Y.-C. Chang, J.-Y. Huang, M.-H. Lee, and C.-S. Chang, Jpn. J. Appl. Phys., Part 1 **48**, 112402 (2009).
[44] Z.-G. Lin, L.-C. Tang, and C.-P. Chou, J. Cryst. Growth **310**, 3224 (2008).
[45] L. Peedikakkandy and P. Bhargava, RSC Adv. **6**, 19857 (2016).
[46] L. Qiu, L. K. Ono, and Y. Qi, Mater. Today Energy **7**, 169 (2018).
[47] Y. Rezaei nik, A. Reyhani, S. Farjami-Shayesteh, and S. Z. Mortazavi, Opt. Mater. **112**, 110754 (2021).
[48] I. Lefebvre, P. E. Lippens, M. Lannoo, and G. Allan, Phys. Rev. B **42**, 9174 (1990).
[49] J. Barrett, S. R. A. Bird, J. D. Donaldson, and J. Silver, J. Chem. Soc. A **0**, 3105 (1971).
[50] P. Hohenberg and W. Kohn, Phys. Rev. **136**, B864 (1964).
[51] W. Kohn and L. J. Sham, Phys. Rev. **140**, A1133 (1965).
[52] M. D. Segall, P. J. D. Lindan, M. J. Probert, C. J. Pickard, P. J. Hasnip, S. J. Clark, and M. C. Payne, J. Phys.: Condens. Matter **14**, 2717 (2002).
[53] P. E. Blöchl, O. Jepsen, and O. K. Andersen, Phys. Rev. B **49**, 16223 (1994).
[54] J. P. Perdew, K. Burke, and M. Ernzerhof, Phys. Rev. Lett. **77**, 3865 (1996).
[55] T. H. Fischer and J. Almlöf, J. Phys. Chem. **96**, 9768 (1992).
[56] H. J. Monkhorst and J. D. Pack, Phys. Rev. B **13**, 5188 (1976).

[57]K. Momma and F. Izumi, J. Appl. Crystallogr. **44**, 1272 (2011).
[58]M. Roknuzzaman, K. (Ken) Ostrikov, K. Chandula Wasalathilake, C. Yan, H. Wang, and T. Tesfamichael, Org. Electron. **59**, 99 (2018).
[59]J. Islam and A. K. M. A. Hossain, RSC Adv. **10**, 7817 (2020).
[60]G. Yu, C. H. Lee, A. J. Heeger, and S.-W. Cheong, Physica C **203**, 419 (1992).
[61]Y. Saeed, B. Amin, H. Khalil, F. Rehman, H. Ali, M. I. Khan, A. Mahmood, and M. Shafiq, RSC Adv. **10**, 17444 (2020).
[62]J. Islam and A. K. M. A. Hossain, Sci. Rep. **10**, 14542 (2020).
[63]X. Liu, B. Xie, C. Duan, Z. Wang, B. Fan, K. Zhang, B. Lin, F. J. M. Colberts, W. Ma, R. A. J. Janssen, F. Huang, and Y. Cao, J. Mater. Chem. A **6**, 395 (2018).
[64]S. Saha, T. P. Sinha, and A. Mookerjee, Phys. Rev. B **62**, 8828 (2000).
[65]M. S. Hossain, M. M. H. Babu, T. Saha, M. S. Hossain, J. Podder, M. S. Rana, M. A. Barik, and P. Rani, AIP Adv. **11**, 055024 (2021).
[66]S. Jana and P. Samal, Phys. Chem. Chem. Phys. **21**, 3002 (2019).
[67]Y. O. Ciftci and M. Evecen, Phase Transitions **91**, 1206 (2018).
[68]J. Wang and Y. Zhou, Phys. Rev. B **69**, 144108 (2004).
[69]S. F. Pugh, London, Edinburgh Dublin Philos. Mag. J. Sci. **45**, 823 (1954).
[70]M. Z. Rahaman and M. A. Islam, J. Supercond. Novel Magn. **34**, 1133 (2021).
[71]H. Fu, D. Li, F. Peng, T. Gao, and X. Cheng, Comput. Mater. Sci. **44**, 774 (2008).
[72]H. Ledbetter and A. Migliori, J. Appl. Phys. **100**, 063516 (2006).
[73]S. I. Ranganathan and M. Ostoja-Starzewski, Phys. Rev. Lett. **101**, 055504 (2008).
[74]R. Gaillac, P. Pullumbi, and F.-X. Coudert, J. Phys.: Condens. Matter **28**, 275201 (2016).